Specular Scattering Probability of Acoustic Phonons in Atomically Flat Interfaces

Yu-Chieh Wen,[1] Chia-Lung Hsieh,[1] Kung-Hsuan Lin,[1] Hung-Pin Chen,[1] Shu-Cheng Chin,[2] Ching-Lien Hsiao,[3] Yuan-Ting Lin,[3] Chia-Seng Chang,[2] Yuan-Chih Chang,[2] Li-Wei Tu,[3] and Chi-Kuang Sun[1,4,*]

[1]*Department of Electrical Engineering and Institute of Photonics and Optoelectronics, National Taiwan University, Taipei 10617, Taiwan*

[2]*Institute of Physics, Academia Sinica, Taipei 115, Taiwan*

[3]*Department of Physics and Center for Nanoscience and Nanotechnology, National Sun Yat-Sen University, Kaohsiung, 80424, Taiwan*

[4]*Research Center for Applied Sciences, Academia Sinica, Taipei 115, Taiwan*

(Received 14 April 2009; revised manuscript received 4 November 2009; published 30 December 2009)

We report a direct determination of the specular scattering probability of acoustic phonons at a crystal boundary by observing the escape of incident *coherent* phonons from the coherent state during reflection. In the sub-THz frequency range where the phonon wavelength is much longer than the lattice constant, the acoustic phonon-interface interaction is found to agree well with the macroscopic theory on wave scattering from rough surfaces. This examination thus quantitatively verifies the dominant role of atomic-scale corrugations in the Kapitza anomaly observed at 1–10 K and further opens a new path to nondestructively estimate subnanoscale roughness of buried interfaces.

DOI: 10.1103/PhysRevLett.103.264301 PACS numbers: 43.35.+d, 44.10.+i

Phonon scattering at a crystal boundary generally causes a reduction in the efficiency of heat transport. At a temperature <1 K, this phenomenon was satisfactorily explained by the acoustic mismatch model, while it deviated from the expectation at higher temperatures (so-called Kapitza anomaly) [1–5]. A number of reports suggested that diffuse scattering of high-frequency phonons (>100 GHz) by interface inhomogeneity or irregularity could be a channel resulting in anomlaous transmission [3]. Even with these studies, no generally accepted theory has emerged due to limited experiments performed with well-characterized interfaces. Consequently, the dominant mechanism inducing the diffuse scattering of high-frequency phonons is still unknown. The corresponding quantitative description of specular (diffuse) scattering probability, the fraction of phonons scattered specularly (diffusively), is thus absent so far. Exploration of these issues is essential not only for explaining present-day observations in cryogenics, but also for heat management in nanoscale devices due to their prominent surface effect.

Transition from normal-to-anomalous Kapitza resistance typically occurs near 1 K up to 10 K, where the dominant acoustic phonons for heat transport have frequencies in the sub-THz range [1–3]. Studies on the corresponding sub-THz acoustic phonon-interface interactions can thus provide critical clues to the cause of Kapitza anomaly. Phonon imaging and phonon-pulse techniques can acquire the information of interface phonon scatterings by examining whether phonon reflection/refraction violates the momentum conservation [2–4], while they cannot determine the specular scattering probability (SSP) quantitatively. In addition, it is difficult to investigate the concerned buried interface with required atomic resolutions during these cryogenic experiments.

In this Letter, we report a direct determination of the SSP of the sub-THz acoustic phonons at well-characterized crystal boundaries. Our quantitative studies indicate the dominant role of atomic-scale interface roughness in diffuse phonon scatterings, which therefore clarify the long-standing debates on Kapitza anomaly. This examination further suggests a new possibility to nondestructively probe subnanoscale corrugations on buried interfaces.

Measurement of the SSP can be realized by looking into the destruction of phonon coherence induced by the diffuse scatterings. The analysis relies on a technique sensitive to phonon phase. Femtosecond laser ultrasonics [5–7] and nanoultrasonics [8–10] can serve as feasible solutions, which detect *only* the coherent part of the acoustic phonons. When photoexcited coherent phonons interact with an interface, the diffuse scatterings cause part of the phonons to be scattered out of the coherent state. Excess reduction in the intensity of scattered coherent phonons compared with the acoustic mismatch model thus reflects the contribution of diffuse scatterings. The SSP is then extracted by monitoring the intensities of the *coherent* acoustic phonons before and after interface scatterings. Few pieces of related literatures with only qualitative analysis or in a lower frequency regime can be found elsewhere [7,9].

Among all of the proposed scattering mechanisms [1], the concern in this Letter is the roughness effect. To correlate the measured SSP with the roughness, the first step is to investigate coherent phonon reflection at solid-air interfaces. The exposure of the concerned interfaces to atmosphere makes high-resolution surface characterizations possible. Moreover, it was known that at solid-vacuum interfaces, loading of liquid helium on solid surfaces did not induce noticeable change in the specular part of reflected phonons [4]. Invariance of the corresponding

SSP suggested that diffuse scattering is mainly related to the properties of solid surfaces rather than the interfacial structure of liquid. It is thus important to clarify the scattering mechanism at *free* solid surfaces for the Kapitza problem. With huge impedance mismatch between air and solid, the excited phonon energy was completely confined in solids so that the dissipation of the coherent phonon intensity during reflection was directly attributed to the diffuse scattering.

Laser-ultrasonic and nanoultrasonic experiments were executed at room temperature with optical pump-probe setups [8]. The light source was a frequency-doubled Ti:sapphire laser with ~200 fs pulse width. The probe wavelength was 365 nm, corresponding to the interband transition of the studied solid medium (GaN), while optical pump pulses with wavelengths of 730 or 365 nm were used for different experiments. Pulse energy and focused spot diameter onto the sample for the blue (infrared) pumps were 0.2 (0.5) nJ and 15 (23) μm. An atomic force microscope (AFM) was used to estimate surface roughness.

Figure 1 shows the schematic diagrams of the experiments for frequency- and roughness-dependent investigations. A heterostructure inside each sample serves as the photoacoustic transducer. The frequency of the generated coherent phonons is in the sub-THz range, corresponding to the typical frequency threshold for anomalous phonon transmission. All samples were epitaxially grown with controllable surface morphology. The diverse distribution of the root-mean-square (rms) roughness σ, ranging from 2 Å (nearly atomic flatness in comparison with the lattice constant $c = 5.2$ Å) to ~10 nm, provides an ideal test platform to examine the roughness effect. Two samples with different structures and σ were adopted to study the phonon scatterings in the low sub-THz regime. One was a GaN-based p-n junction [Fig. 1(a)] with an atomic-level flat surface ($\sigma = 0.68 \pm 0.2$ nm). Sample details were reported before [6]. The other was a 1 μm-thick GaN thin film grown on a Si(111) wafer, as shown in Fig. 1(b). By manipulating growth condition, this epilayer has an irregular surface with $\sigma = 8.2 \pm 1.7$ nm.

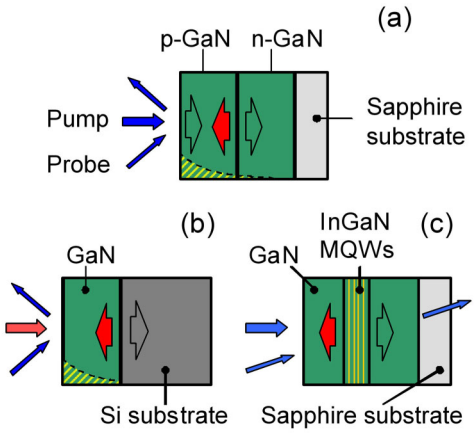

FIG. 1 (color online). Schematic diagrams of the studied samples. Arrows in each sample depict the propagation of the generated acoustic phonons, and one of them (toward the surface) is adopted for investigating phonon-boundary interactions. The photoacoustic detection regions inside the samples are represented by the dashed area.

Figures 2(a) and 2(b) show the measured transient optical reflectivities in these low-frequency samples, where the charged-carrier background was removed for clarity. Clear Brillouin oscillations in the extracted signals are the indication of the detected 117 GHz coherent phonons which are the component of the excited broadband phonon pulses satisfying the optical interference condition. After photoexciting the p-n junction by blue pumps [Fig. 2(a)], part of the 117 GHz coherent phonons initiated in the depletion region traveled toward the sample surface and then reflected back toward the substrate at ~150 ps. With a limited surface detection region, the round-trip of transport phonons resulted in a symmetric envelope (dashed lines) with a maximum at ~150 ps. High symmetry of this envelope revealed that the coherent phonon intensity was almost unchanged after surface reflection, indicating a SSP near unity (0.99 ± 0.01). The rest part of the signal exhibited an

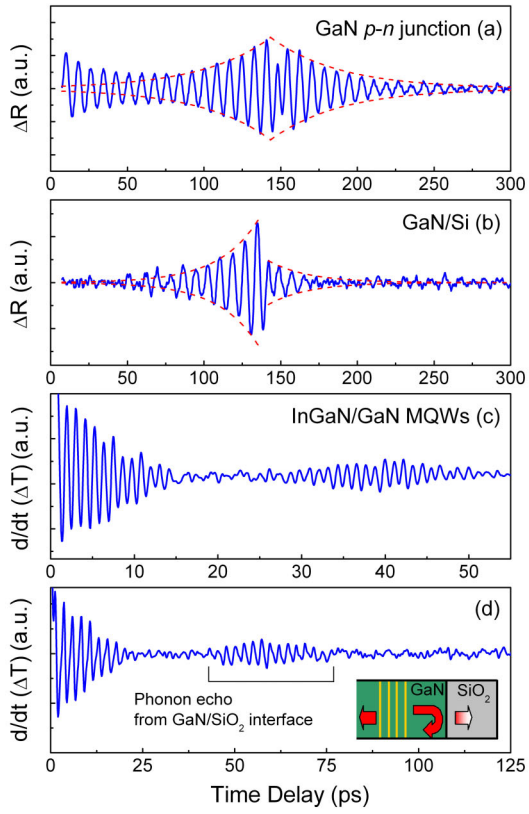

FIG. 2 (color online). (a), (b) Extracted transient optical reflectivity (solid lines) measured with a GaN p-n junction and a GaN/Si epilayer. The concerned features of phonon reflection are depicted as dashed lines. (c), (d) Differential transient transmission changes obtained in a 14-period InGaN/GaN MQW and a 10-period InGaN/GaN MQW with a SiO_2 cap layer. Related technical details can be found elsewhere [6,8].

initial damped oscillation, which was contributed from the departure of coherent phonons generated by the screening of the surface field.

As for the rough GaN/Si sample [Fig. 2(b)], coherent phonons were generated from the Si/GaN boundary by absorbing infrared pumps. With the same detection condition, the identical frequency component of the excited phonons was monitored before and after reflection at the GaN/air surface (~140 ps). The abrupt drop in the envelope amplitude during the surface reflection revealed a low SSP of 0.132. Compared with the result of the flat *p-n* junction sample, the observed serious diffuse scatterings at this sample surface is thus ascribed to the interface corrugations. With a Planck distribution of thermal phonons, 117 GHz phonons correspond to the dominant heat carriers at 1.3 K. It is near the typical temperature threshold for the transition of normal-to-anomalous Kapitza resistance [1]. The above experiments thus demonstrated the significant effect of nanometer roughness on the thermal conduction at this key temperature.

Figure 1(c) illustrates the nanoultrasonic examination on the roughness effect in the high sub-THz regime. In this sample, generation and detection of the coherent acoustic phonons were achieved by 14-period 36 Å/43 Å InGaN/GaN multiple quantum wells (MQWs) [10]. Here, the studied phonon wavelength λ is determined by the period of MQWs. The initial acoustic phase front is assumed to be perfectly plane based on the confirmed quality of the MQWs, the fact that the coherent phonons were generated following the electron wave function distribution in 14 QWs, and the characteristic of narrow-band analysis [8]. This heterostructure enabled us to explore the interaction between high-frequency phonons (890 GHz, corresponding to the peak phonon population at ~10 K) and epitaxial surfaces ($\sigma = 0.68 \sim 1.2$ nm). The location variation in σ was originated from the inhomogeneity of the growth condition. Taking advantage of this position-dependent property, the correlation between high-frequency phonon scatterings and the atomic-scale roughness was studied in detail through performing *in situ* AFM and optical measurements on different locations of this sample.

Figure 2(c) shows an example of the experimental traces taken at a surface spot with $\sigma = 0.82$ nm using 390 nm optical wavelength. Transient optical transmission was recorded, revealing phonon-modulated light absorption in the QWs. The coherent phonon oscillations were found to be within the first 15 ps and between 25–55 ps. The earlier one was due to the propagation of the photoexcited phonons out of the MQWs, and the later one was induced by the coherent phonon echo reflected from the sample surface. A previous study in GaN [10] had estimated the temperature-dependent propagation loss, which at room temperature was dominated by the anharmonic scatterings. By comparing the amplitudes of these two coherent phonon oscillations and calibrating the propagation loss, the SSP at this specific surface point can be extracted to be ~0.45. The high-frequency measurements on different locations concluded that the SSP value decreased from 0.62 to 0.17 when the σ increased from 0.68 to 1.2 nm. This trend is qualitatively consistent with the 117 GHz data, as summarized in Fig. 3. Furthermore, it was noticed that phonons with a higher frequency are much more responsive to the atomic-scale roughness. This fact is disclosed not only by the observed steep increase in the diffuse scattering probability of 890 GHz phonons under a slight increase in σ (0.68–1.2 nm) but also by a remarkable difference in diffuse scatterings (1% versus 38%) between 117 and 890 GHz results with a similar σ of ~0.68 nm.

These experiments qualitatively exhibited a strong connection between sub-THz phonon scattering and surface irregularity. To understand these data, acoustic phonon-boundary interactions were then analyzed theoretically. With flat surfaces ($\sigma/\lambda < 0.15$) and long phonon wavelengths ($\lambda/c > 15$), phonon transport can be treated as wave propagation in continuum media. It is analogous to the continuum acoustic theory adopted in the explanation of heat transport in the low-temperature regime ($\ll$1 K), while the scattering by interface roughness is our concern. Thus, the studied phase-related scattering issue can be modeled as classical waves scattered from rough surfaces. We considered the small slope approximation (SSA) due to its accuracy even with a broad range of scattering angles [11]. The roughness spectrum $W(K)$ used in the SSA analysis is the modified power law spectrum given by

$$W(K) = \frac{A}{(K^2 l^2 + 1)^2}, \tag{1}$$

where $A = 2\sigma^2 l/\pi$ is the spectral strength, and K and l are the wave number and the correlation length of surface roughness, respectively. By introducing the corresponding

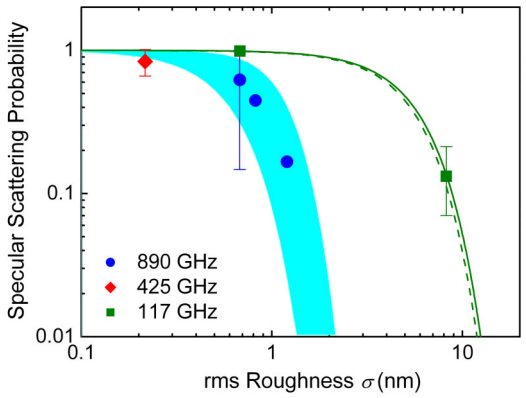

FIG. 3 (color online). Specular scattering probability (SSP) as a function of σ measured in four uncapped samples (dots). The 890 GHz data were obtained on different locations of a specific sample, while the other low-frequency data were taken from different samples. The solid (dashed) line depicts the SSA prediction for the scatterings of 117 GHz phonons at the GaN *p-n* junction (GaN/Si) sample surface where $l = 24(38)$ nm, while the same theoretical investigation for 890 GHz phonons is represented by the ranged area due to uncertainty in l.

correlation function into the lowest-order nonlocal SSA, one can obtain the coherent reflection coefficient r formulated in terms of σ, l, phonon wave vector k, and the reflection coefficient for a perfectly smooth interface r_0 [12]. It is important to know that $(r/r_0)^2$ reveals the intensity loss of the reflected coherent waves and represents the SSP of incident phonons from a particle viewpoint.

Besides the measurement results, Fig. 3 illustrates the corresponding predictions from the SSA. With $r_0 = 1$, the measured l and the normal incidence condition were introduced in the calculation. l was estimated to be 24 (38) nm for the p-n junction (GaN/Si) sample. As for the MQW sample, the SSA analysis with such a short λ (7.9 nm) strongly depends on nanoscale lateral characteristic of the roughness. Without required precision for the determination of l, the SSA provides a ranged prediction for 890 GHz phonons with the consideration of $l \gg$ or $\ll \lambda$. From the figure, the experimental results are found to be satisfactorily consistent with the wave scattering theory. It should be noted that without considering other scattering channels, the SSA calculation concerning only the roughness effect gives the upper bound of the SSP. The quantitative agreement between the theory and the measurements thus shows the fact that interface roughness dominates over other scattering mechanisms for phonon-boundary interactions in the sub-THz frequency range.

Both theory and experiments indicate a specular-to-diffuse transition of phonon scatterings as the surface (frequency) becomes irregular (higher). Our finding facilitates the understanding of the cryogenic heat transport. By considering the properties of typical solid-state surface with σ of 1–10 nm and sound velocities of 4–8 nm/ps, the threshold phonon frequency for the specular-to-diffuse transition, defined by SSP $= 0.5$, can be evaluated to range from several tens to hundreds of GHz. Acoustic phonons in this frequency range govern the thermal conduction at 0.3–10 K. This calculated transition frequency/temperature based on the roughness effect agrees with the reported cryogenic observations on Kapitza anomaly [1–3].

One datum (425 GHz) shown in Fig. 3 should be especially addressed since it was measured with an extremely flat surface ($\sigma \sim 2$ Å, less than the thickness of one monolayer). Without notable irregularity, this datum confirmed the predominance of the specular scatterings at nearly perfect surfaces. Furthermore, the same epitaxial sample was then used to examine the validity of the above conclusion for interfaces between two media. We coated a 330-nm-thick SiO_2 cap layer on this sample, and the transmission electron microscopy confirmed the atomically flat and well-bonded interface between GaN and SiO_2. The estimated interface roughness was less than one lattice constant of GaN ($\sigma < c$), thus yielding low roughness-induced diffuse scatterings according to the SSA ($r/r_0 > 0.89$). With such negligible roughness contribution, the effects of other scattering mechanisms at buried interfaces [1] should then be revealed by performing nanoultrasonic experiments [Fig. 2(d)]. The measured coherent reflection coefficient of this GaN/SiO_2 interface for 425 GHz phonons is $r/r_0 = 0.91 \pm 0.08$, where $r_0 = 0.575$–0.602 with consideration of uncertainty in the sound velocity of bulk SiO_2 [13]. The reasonable agreement between the experiment and the roughness-based scattering theory indicates that no noticeable diffuse scattering is induced by other mechanisms. It thus supports the responsible role of roughness in interface diffuse scatterings, as well as in the anomalous phonon transmission through an interface.

From an application point of view, our finding leads a way to *nondestructively* probe corrugations of *buried* interfaces with atomic resolutions, compared with nowadays surface or destructive nanometrologies. The experiment shown in Fig. 2(d) also serves as a demonstration of the proposed nanoultrasonic-based technique, where σ of the GaN/SiO_2 interface can be estimated by analyzing scattering of the acoustic phonons with the SSA model.

In summary, we report a direct measurement of the SSP of acoustic phonons at epitaxial interfaces. Our observations *quantitatively* verify that the interface diffuse scattering of sub-THz transport phonons is mainly induced by roughness, which is thus concluded as the dominant mechanism responsible for Kapitza anomaly. This exploration on microscopic phonon-boundary interactions is essential for explaining nowadays observations in cryogenics and further opens a path for noninvasive probing of nanoscale interface irregularity.

The authors appreciate J.-K. Wang and S.-B. Wu for providing technical support and also thank O. B. Wright and T.-M. Liu for inspiring scientific discussions. The samples were kindly provided by S. Keller, S. P. DenBaars, and J.-I. Chyi. This work was sponsored by the National Science Council of Taiwan under Grant No. NSC-98-2120-M-002-001 and MediaTek.

*sun@cc.ee.ntu.edu.tw

[1] E. T. Swartz and R. O. Pohl, Rev. Mod. Phys. **61**, 605 (1989).
[2] G. A. Northrop and J. P. Wolfe, Phys. Rev. Lett. **52**, 2156 (1984).
[3] J. Weber *et al.*, Phys. Rev. Lett. **40**, 1469 (1978).
[4] P. Taborek and D. L. Goodstein, Phys. Rev. B **22**, 1550 (1980).
[5] G. Tas and H. J. Maris, Phys. Rev. B **55**, 1852 (1997).
[6] K.-H. Lin *et al.*, Appl. Phys. Lett. **86**, 093110 (2005).
[7] C. Rossignol *et al.*, J. Appl. Phys. **95**, 4157 (2004).
[8] K.-H. Lin *et al.*, Nature Nanotech. **2**, 704 (2007).
[9] C.-L. Hsieh *et al.*, Appl. Phys. Lett. **85**, 4735 (2004).
[10] T.-M. Liu *et al.*, Appl. Phys. Lett. **90**, 041902 (2007).
[11] S. L. Broschat and E. I. Thorsos, J. Acoust. Soc. Am. **101**, 2615 (1997).
[12] S. L. Broschat, IEEE Transactions on Geoscience and Remote Sensing **37**, 632 (1999).
[13] O. Matsuda *et al.*, Phys. Rev. B **77**, 224110 (2008).